Supplementary Information

Synthesis, Photophysical Behavior, DFT Analysis, Electrochemical and Investigative Optical Sensor Properties of C3-Functionalized 4-Hydroxycoumarins

Amanda de A. Borges,[a] Jenifer L. da Rosa,[b] Yuri P. V. de Carvalho,[a] Vitor F. Ferreira,[c] Fernando de C. da Silva,[a] Paulo C. Piquini,[b] Bernardo A. Iglesias*,[d] and Luana da S. M. Forezi*,[a]

[a]Laboratório de Síntese Orgânica Aplicada, Instituto de Química, Universidade Federal Fluminense, 24020-141 Niterói-RJ, Brazil

[b]Departamento de Física, Universidade Federal de Santa Maria, 97105-900 Santa Maria-RS, Brazil

[c]Faculdade de Farmácia, Universidade Federal Fluminense, 24241-002 Niterói-RJ, Brazil

[d]Departamento de Química, Universidade Federal de Santa Catarina, 88040-900 Florianópolis-SC, Brazil

*e-mail: luanaforezi@id.uff.br; bernardo.iglesias@ufsc.br

This publication is part of the special issue “Organic Synthesis - BMOS”

Amanda de A. Borges: https://orcid.org/0009-0006-9744-1532
Yuri P. V. de Carvalho: https://orcid.org/0009-0004-9338-8899
Vitor F. Ferreira: https://orcid.org/0000-0002-2166-766X
Fernando de C. da Silva: https://orcid.org/0000-0002-2042-3778
Paulo C. Piquini: https://orcid.org/0000-0003-4340-2723
Bernardo A. Iglesias: https://orcid.org/0000-0002-4039-6316
Luana da S. M. Forezi: https://orcid.org/0000-0002-7657-4268

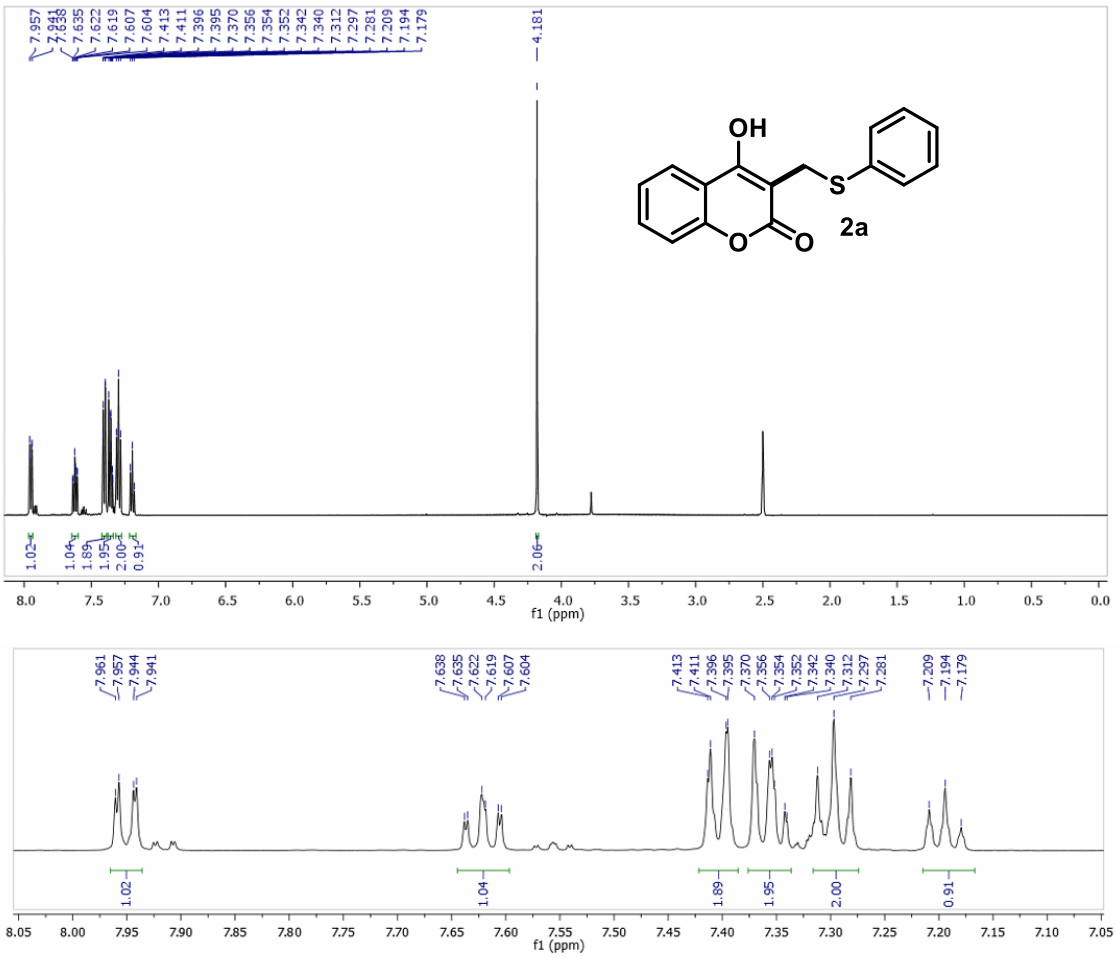

Figure S1. ^{1}H NMR spectrum (500 MHz, DMSO-d_6) of **2a**.

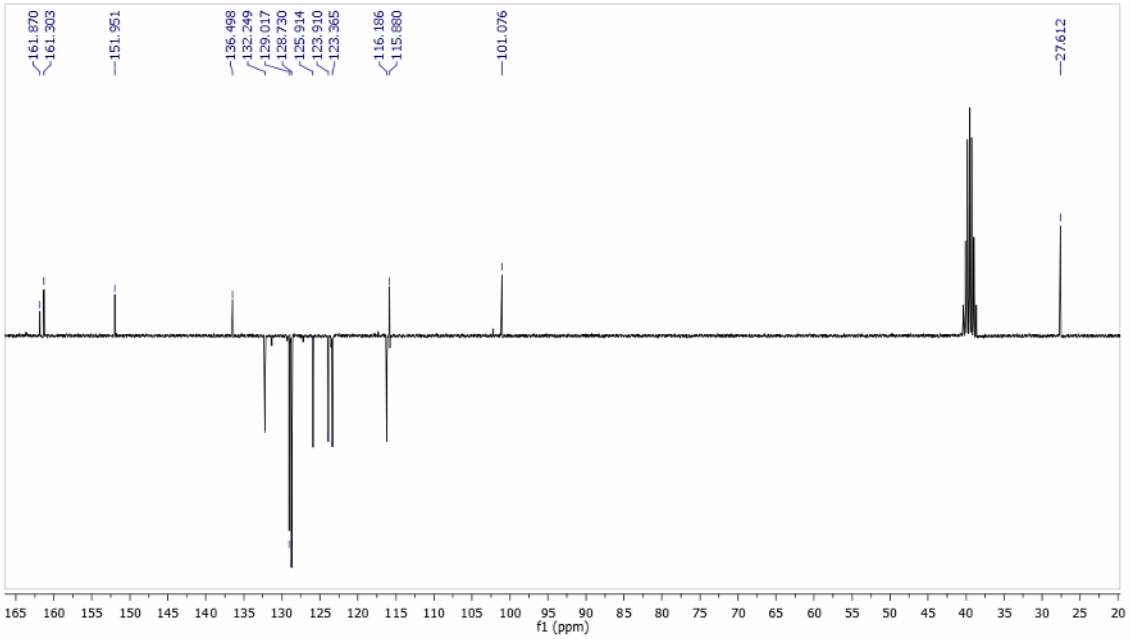

Figure S2. ^{13}C NMR spectrum (125 MHz, DMSO-d_6) of **2a**.

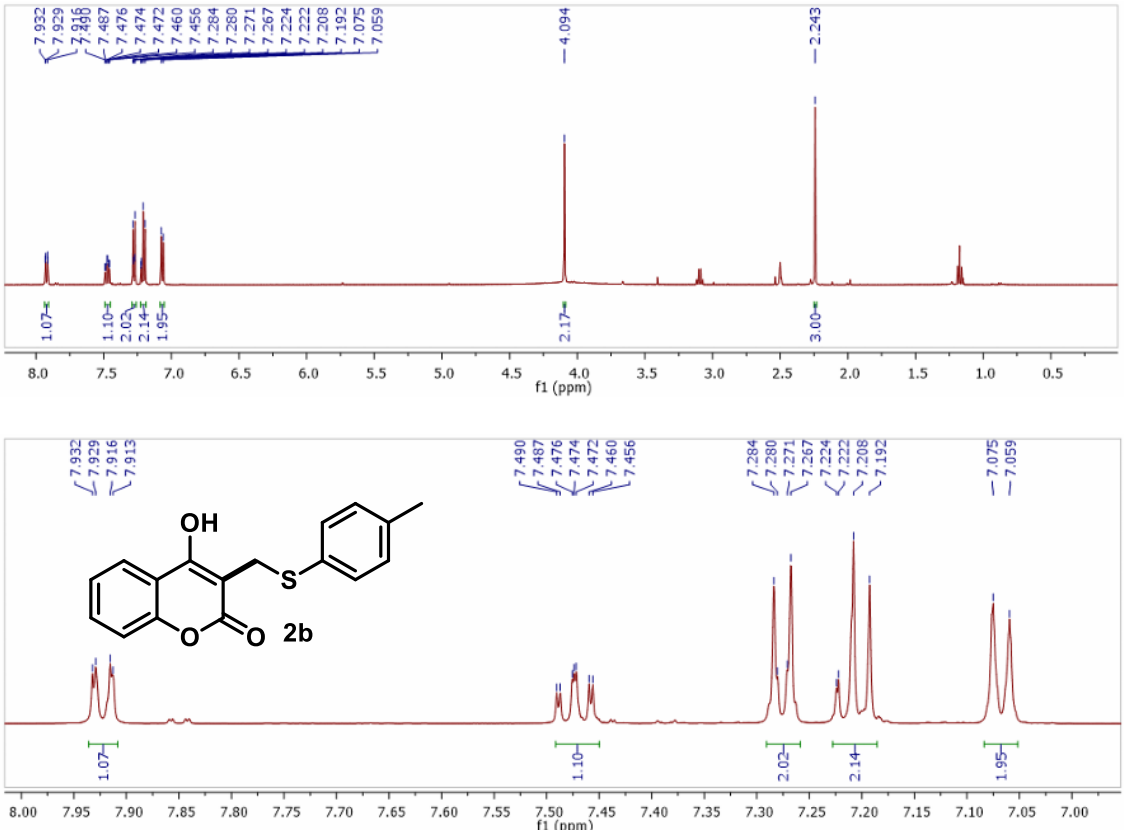

Figure S3. ^{1}H NMR spectrum (500 MHz, DMSO-d_6) of **2b**.

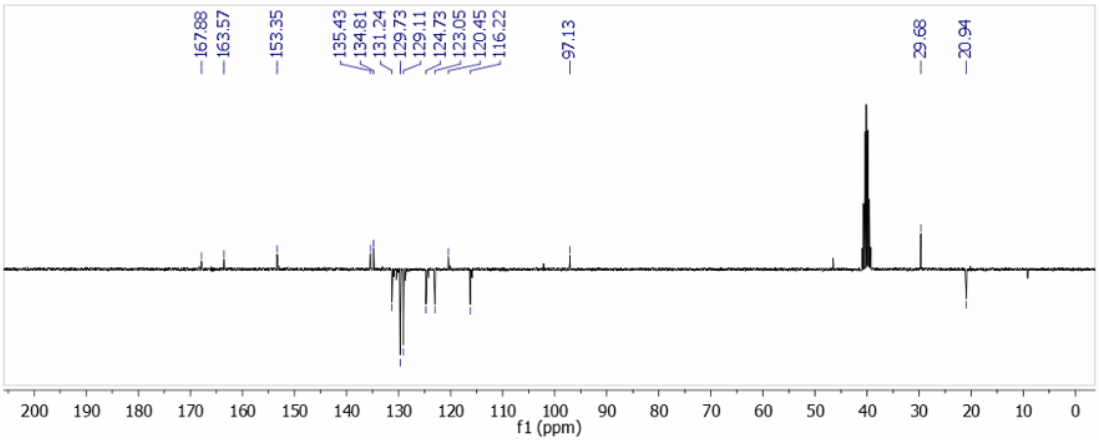

Figure S4. ^{13}C NMR spectrum (125 MHz, DMSO-d_6) of **2b**.

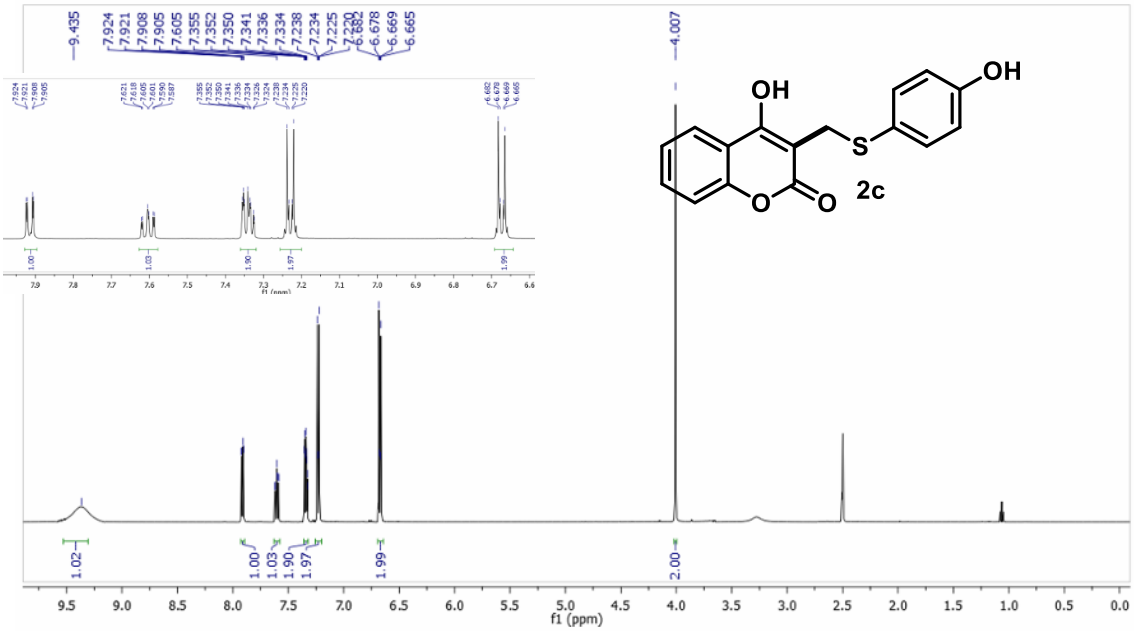

Figure S5. ^{1}H NMR spectrum (500 MHz, DMSO-d_6) of **2c**.

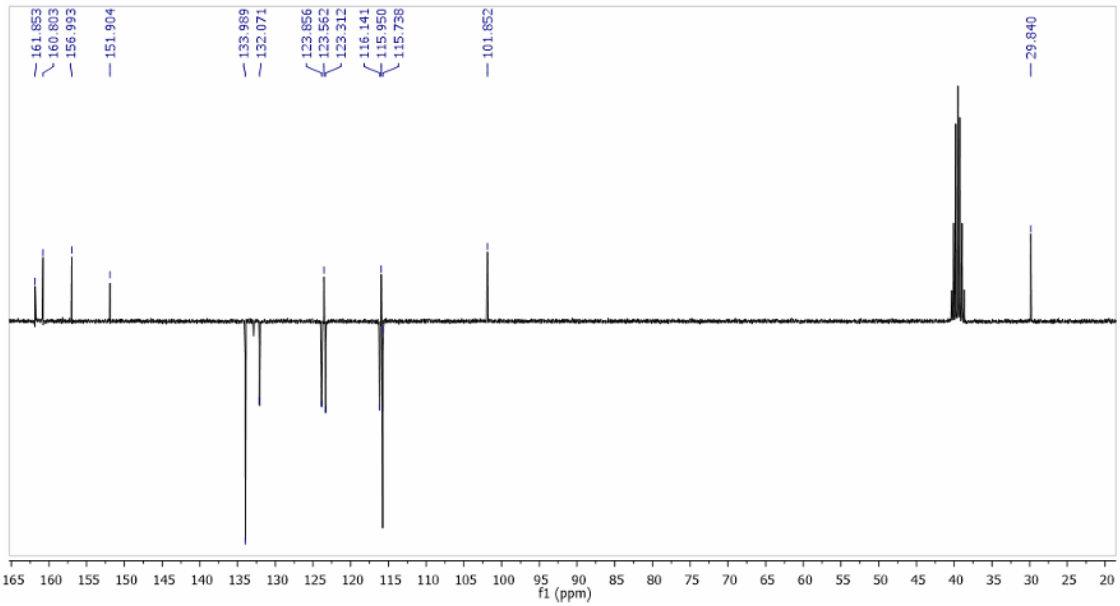

Figure S6. ^{13}C NMR spectrum (125 MHz, DMSO-d_6) of **2c**.

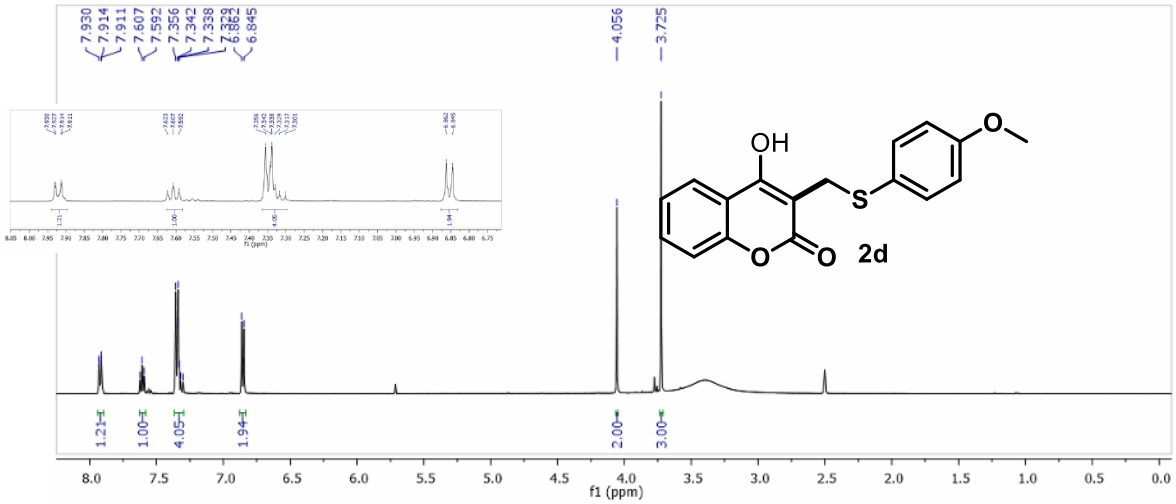

Figure S7. ^{1}H NMR spectrum (500 MHz, DMSO-d_6) of **2d**.

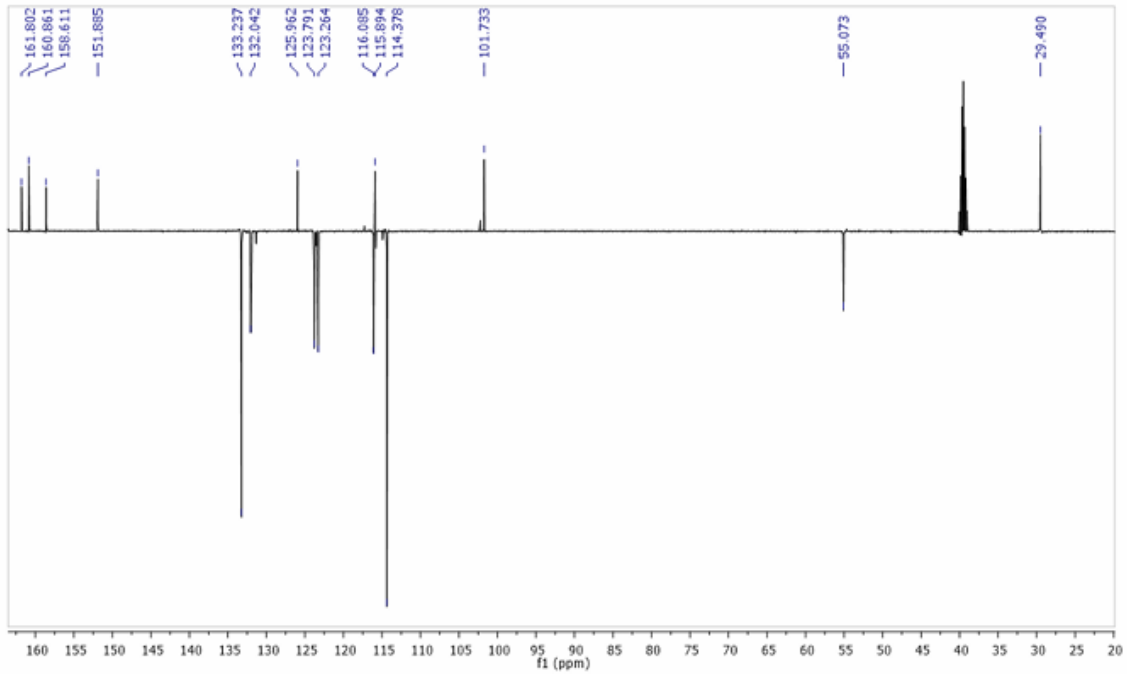

Figure S8. ^{13}C NMR spectrum (125 MHz, DMSO-d_6) of **2d**.

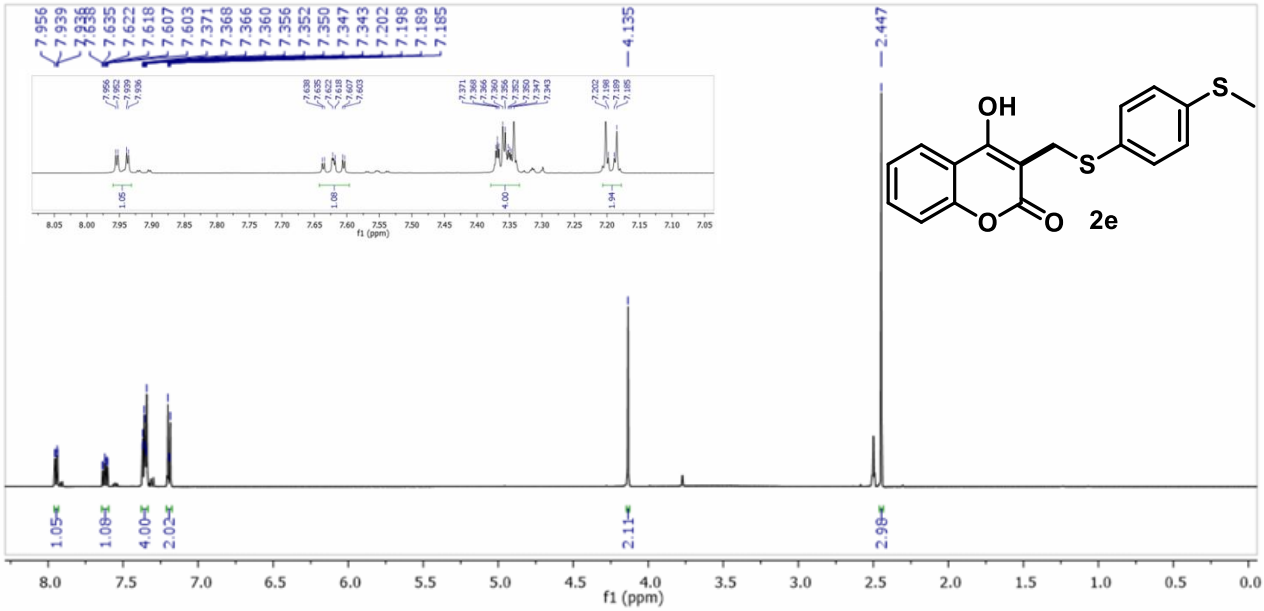

Figure S9. ^{1}H NMR spectrum (500 MHz, DMSO-d_6) of **2e**.

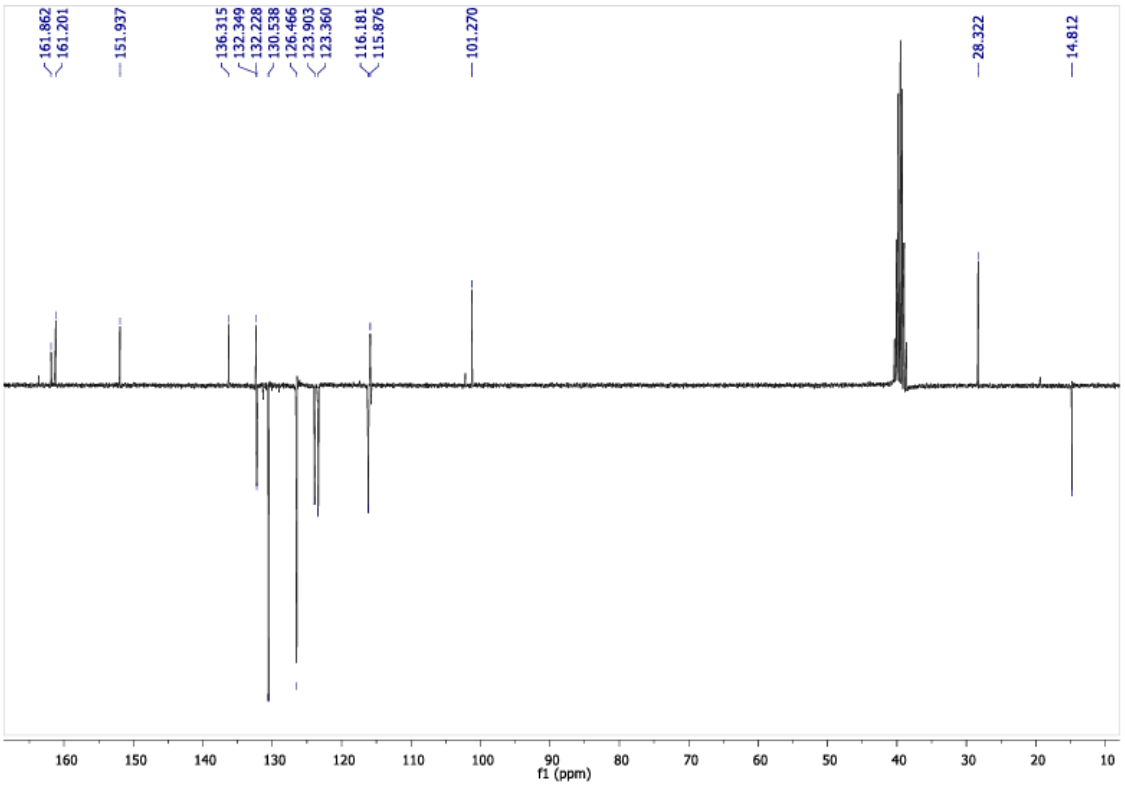

Figure S10. ^{13}C NMR spectrum (125 MHz, DMSO-d_6) of **2e**.

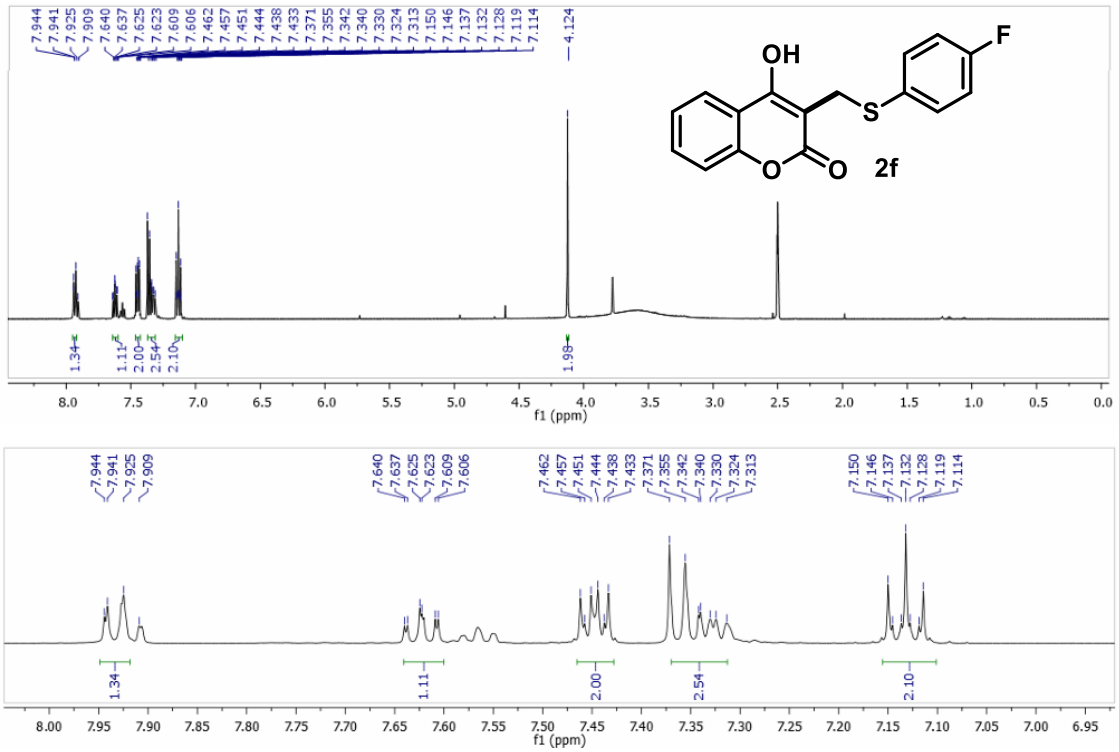

Figure S11. ^{1}H NMR spectrum (500 MHz, DMSO-d_6) of **2f**.

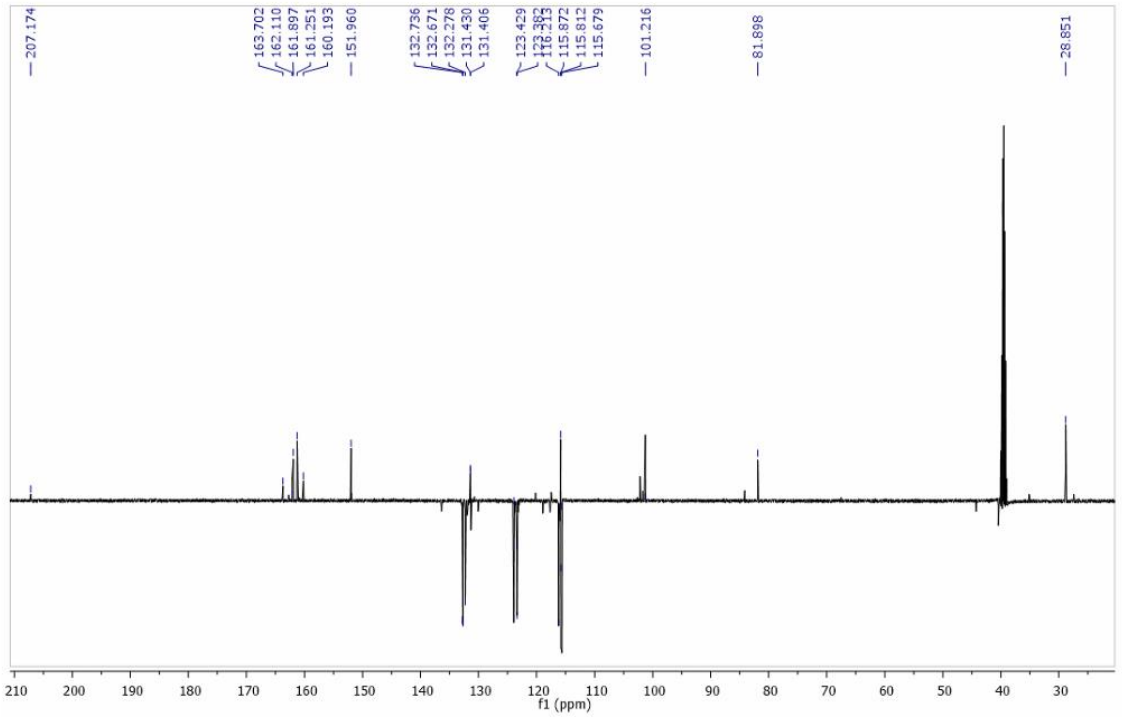

Figure S12. ^{13}C NMR spectrum (125 MHz, DMSO-d_6) of **2f**.

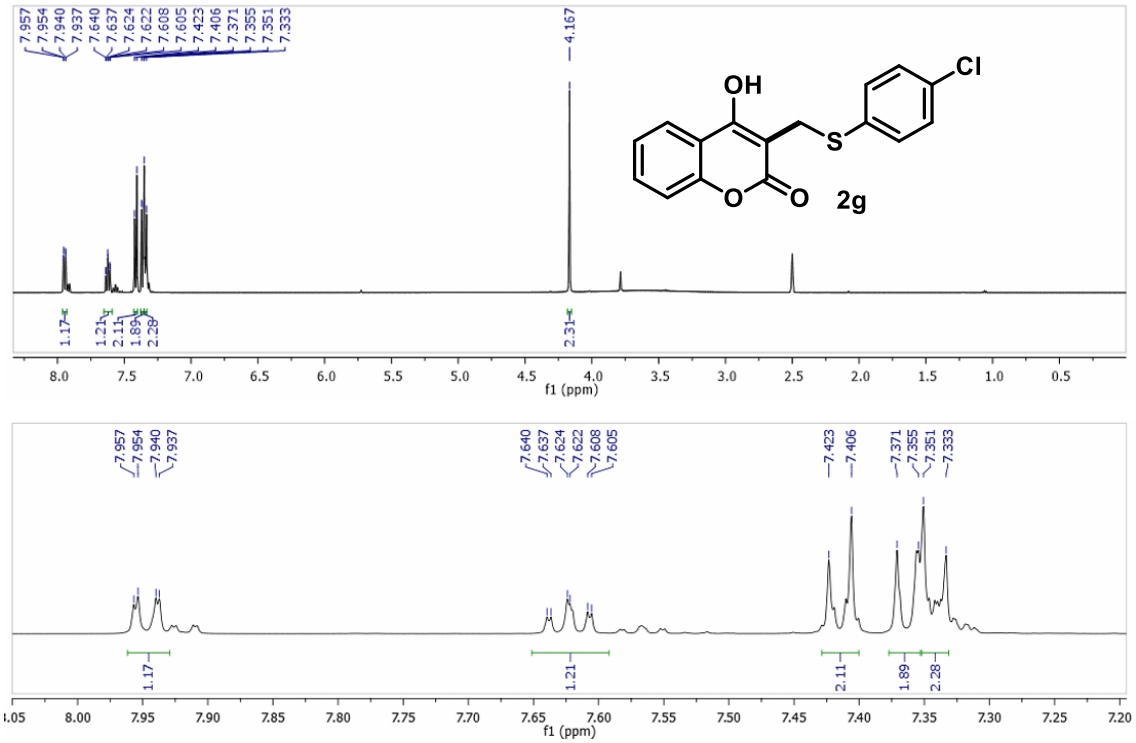

Figure S13. ^{1}H NMR spectrum (500 MHz, DMSO-d_6) of **2g**.

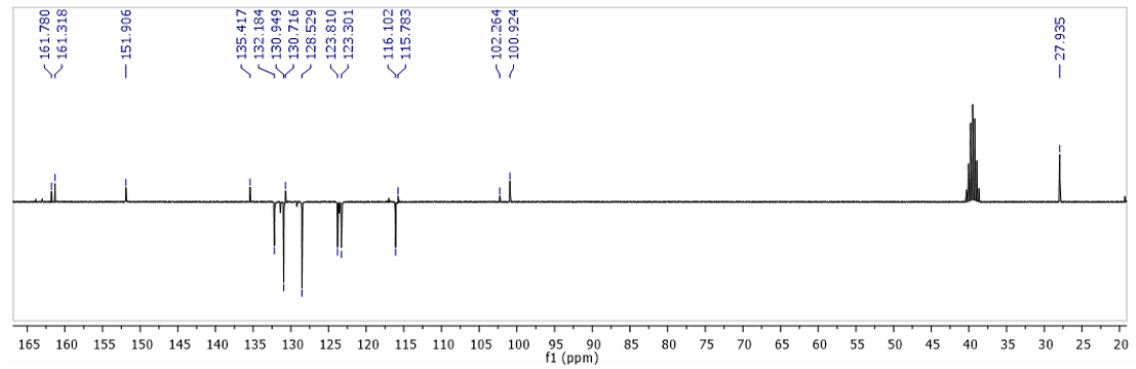

Figure S14. ^{13}C NMR spectrum (125 MHz, DMSO-d_6) of **2g**.

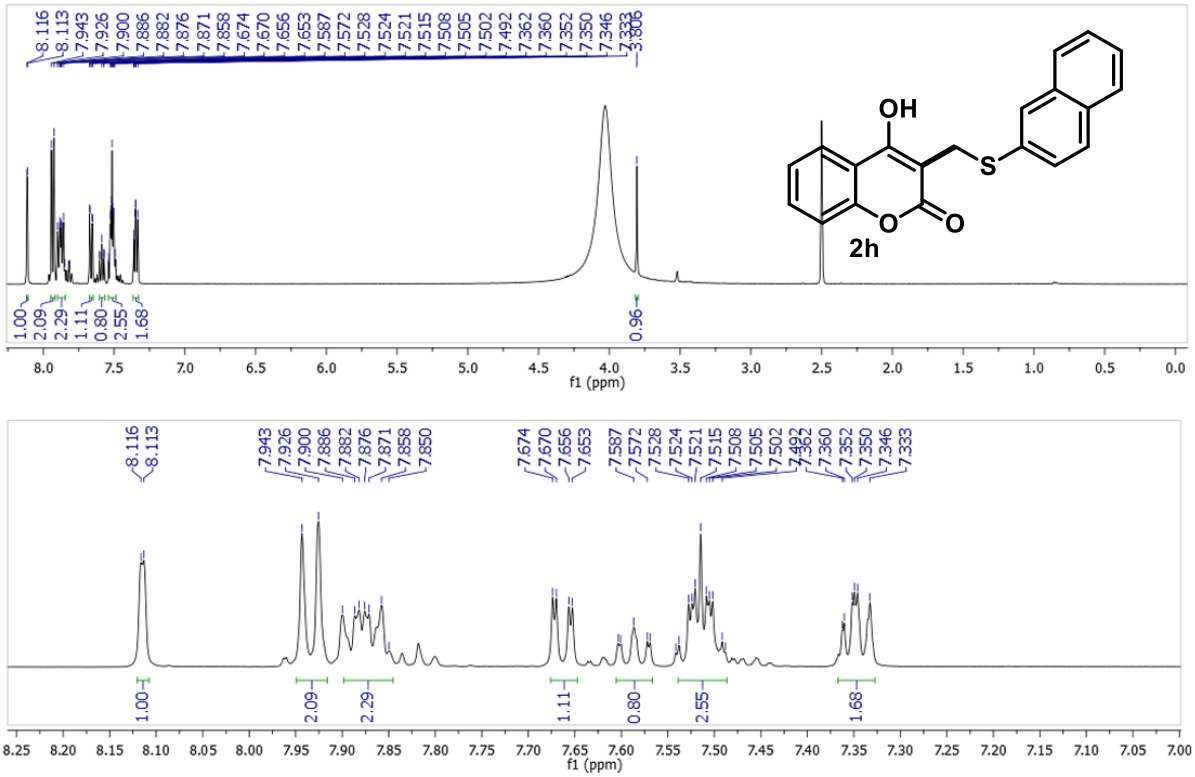

Figure S15. ^{1}H NMR spectrum (500 MHz, DMSO-d_6) of **2h**.

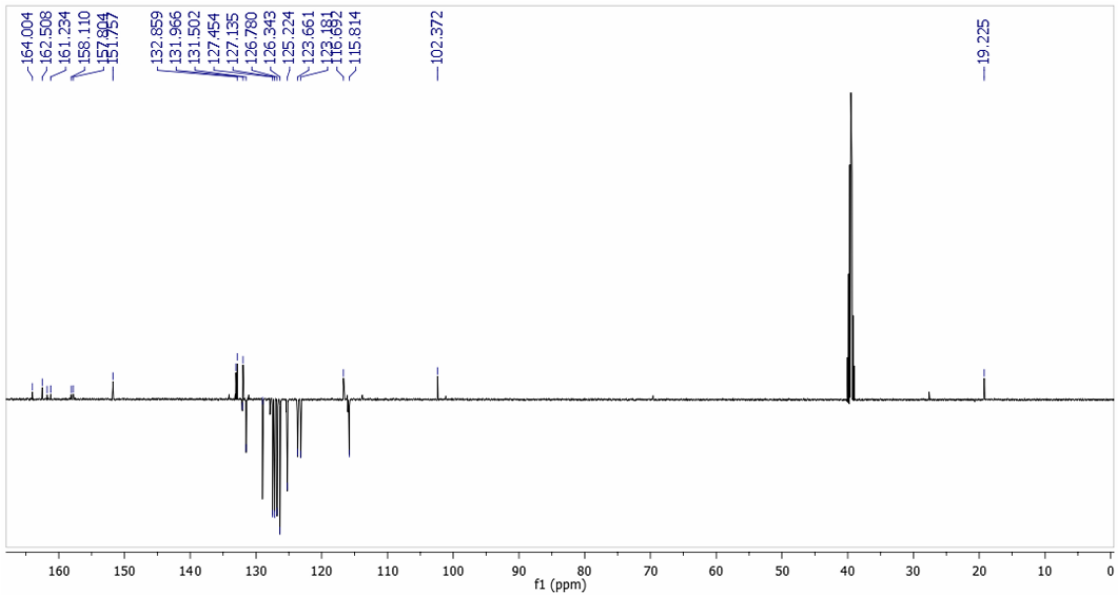

Figure S16. ^{13}C NMR spectrum (125 MHz, DMSO-d_6) of **2h**.

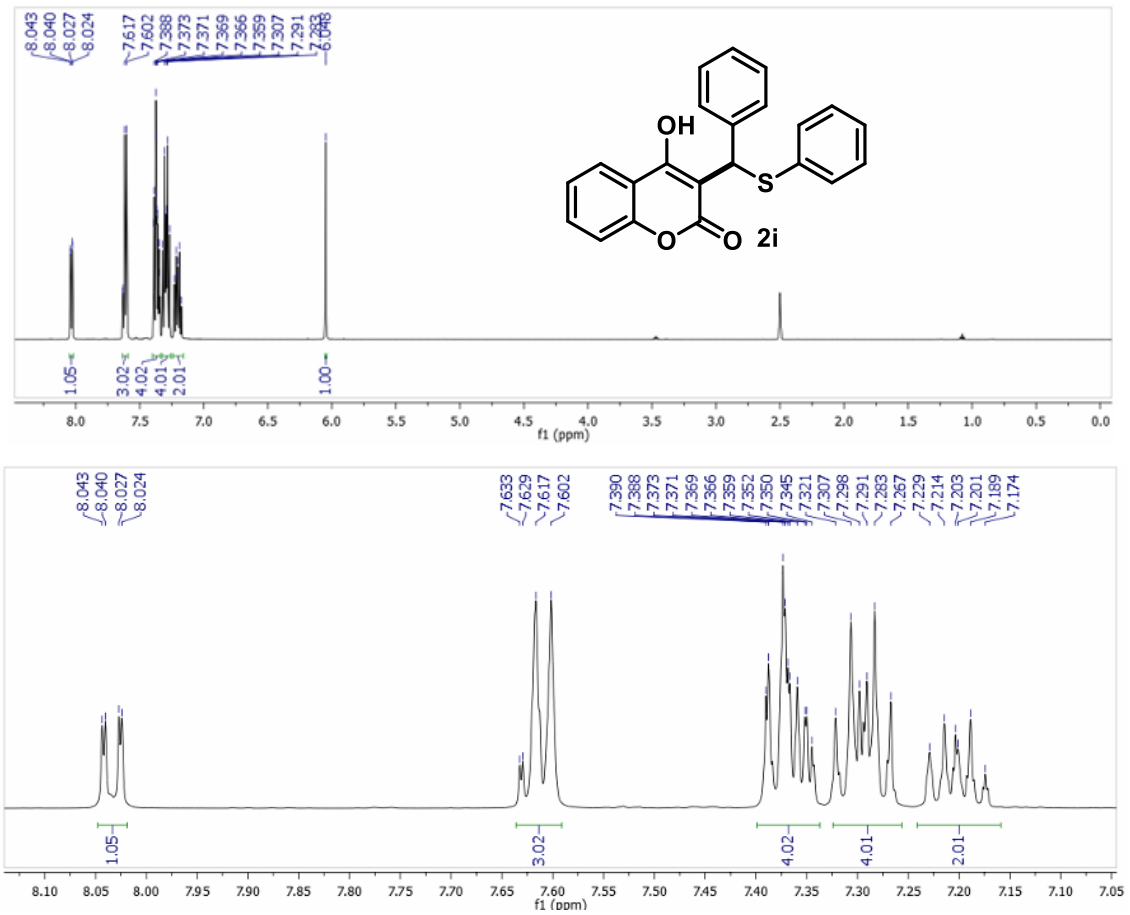

Figure S17. ^{1}H NMR spectrum (500 MHz, DMSO-d_6) of **2i**.

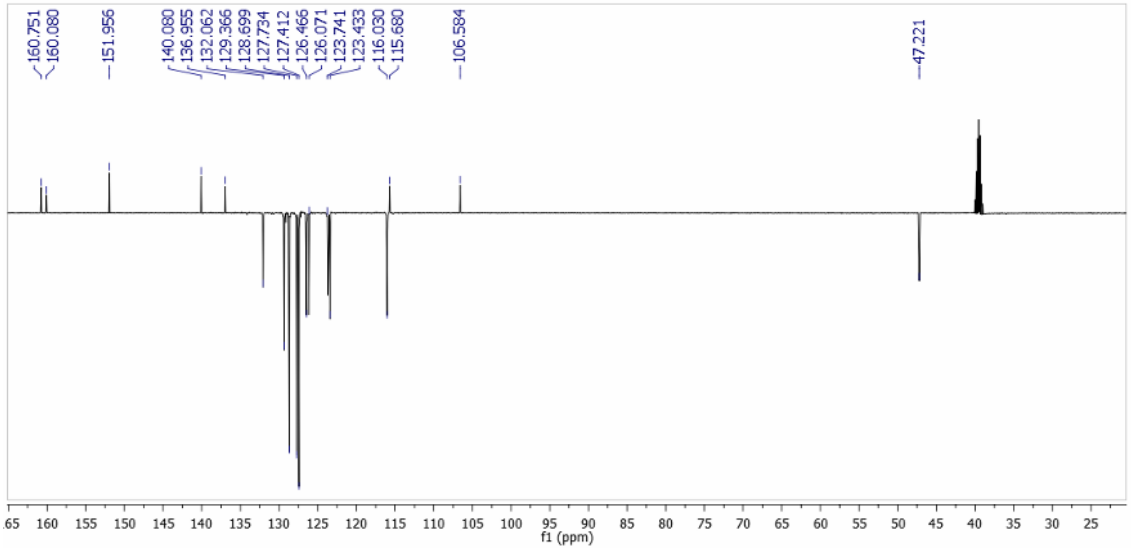

Figure S18. ^{13}C NMR spectrum (125 MHz, DMSO-d_6) of **2i**.

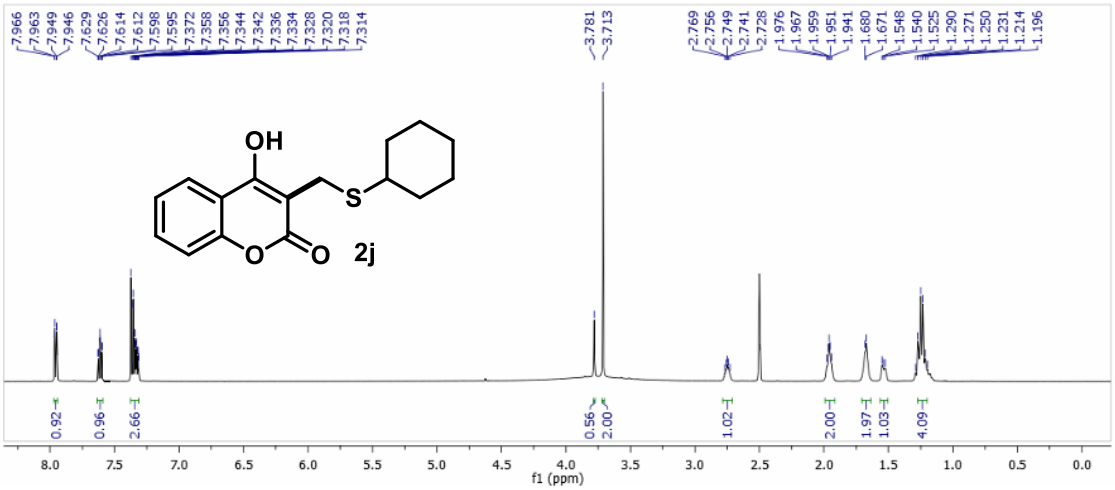

Figure S19. ^{1}H NMR spectrum (500 MHz, DMSO-d_6) of **2j**.

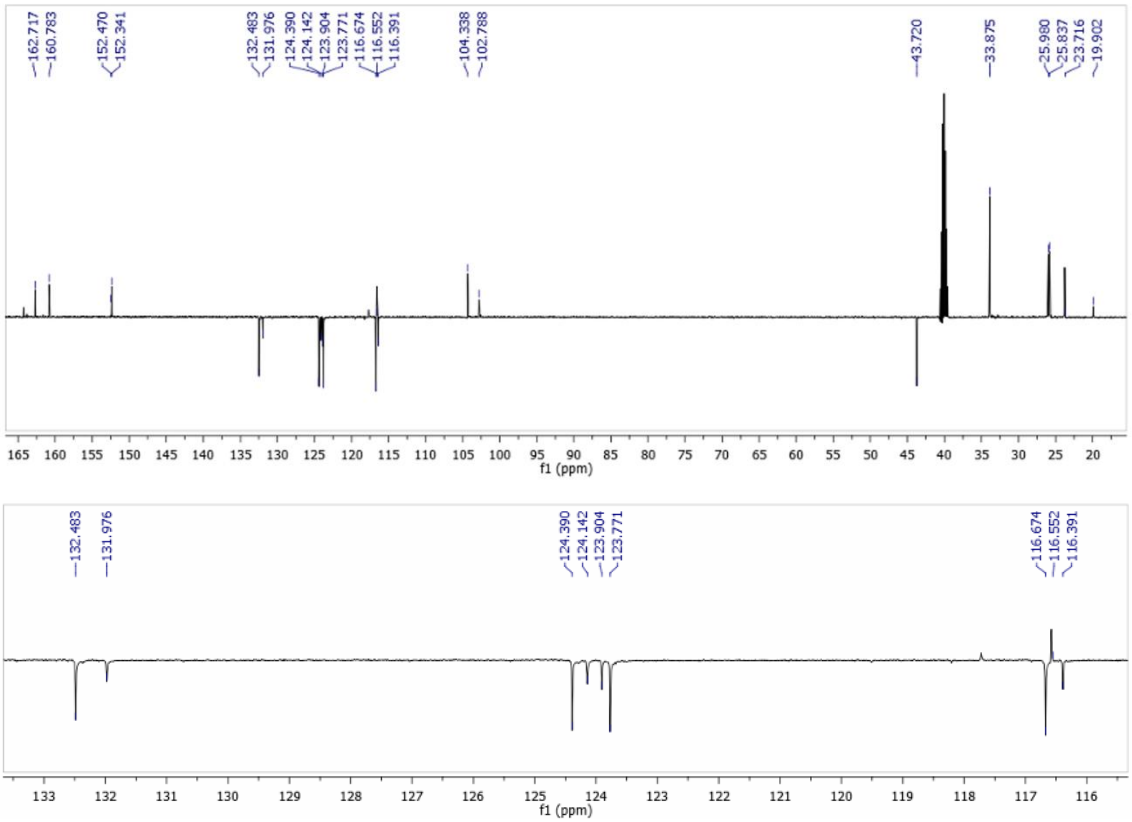

Figure S20. ^{13}C NMR spectrum (125 MHz, DMSO-d_6) of **2j**.

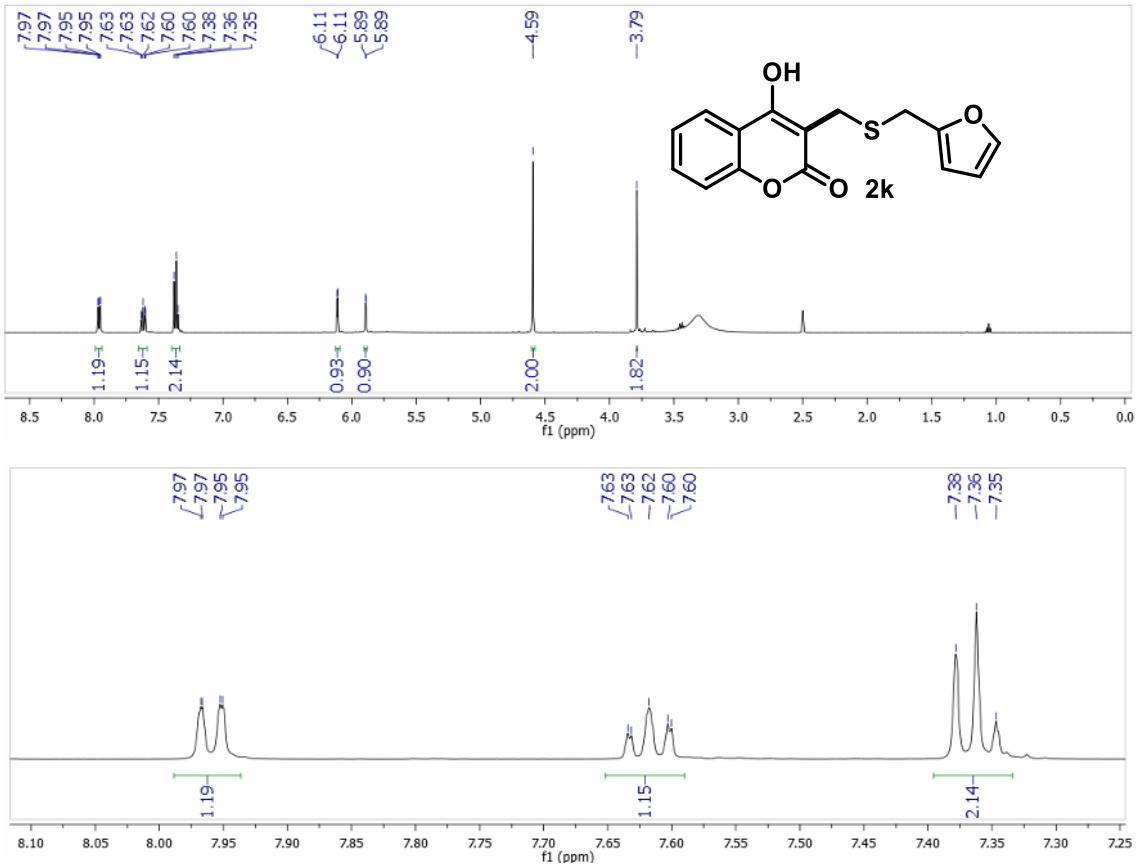

Figure S21. ^{1}H NMR spectrum (500 MHz, DMSO-d_6) of **2k**.

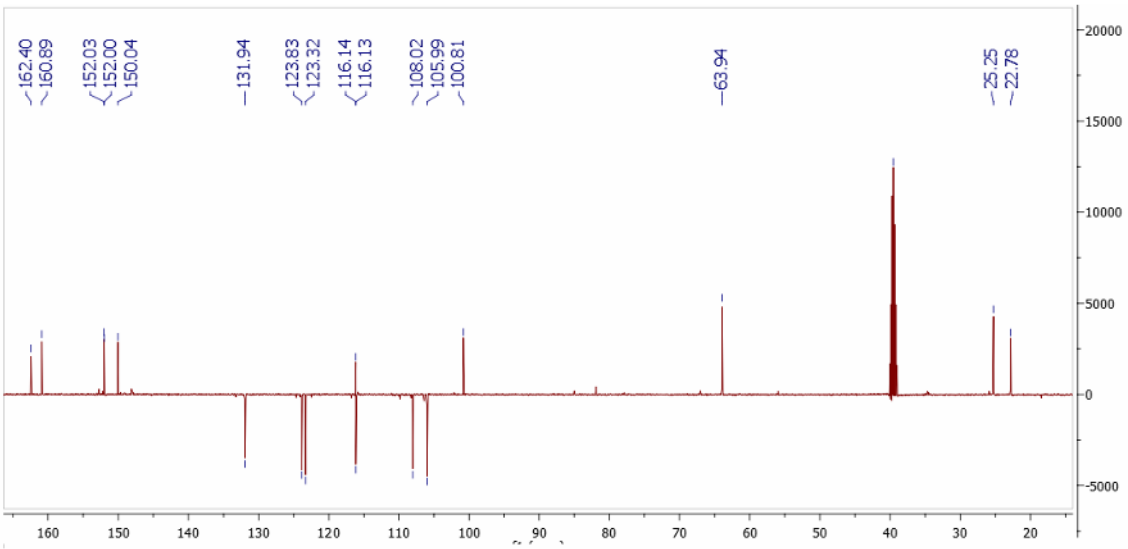

Figure S22. ^{13}C NMR spectrum (125 MHz, DMSO-d_6) of **2k**.

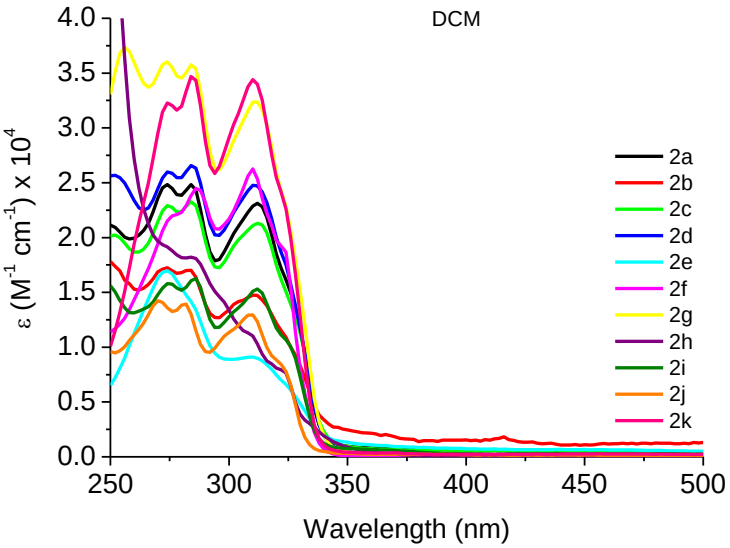

Figure S23. UV-Vis absorption spectra of coumarin derivatives **2a-2k** in DCM (fixed concentration at 20 μM).

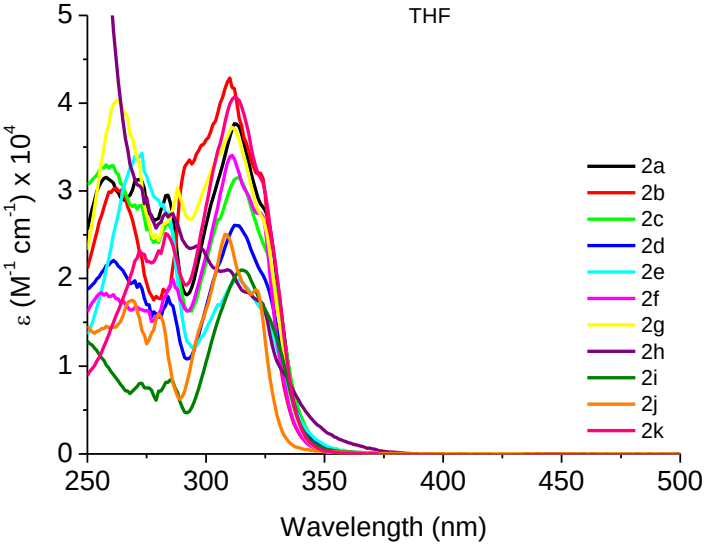

Figure S24. UV-Vis absorption spectra of coumarin derivatives **2a-2k** in THF (fixed concentration at 20 μM).

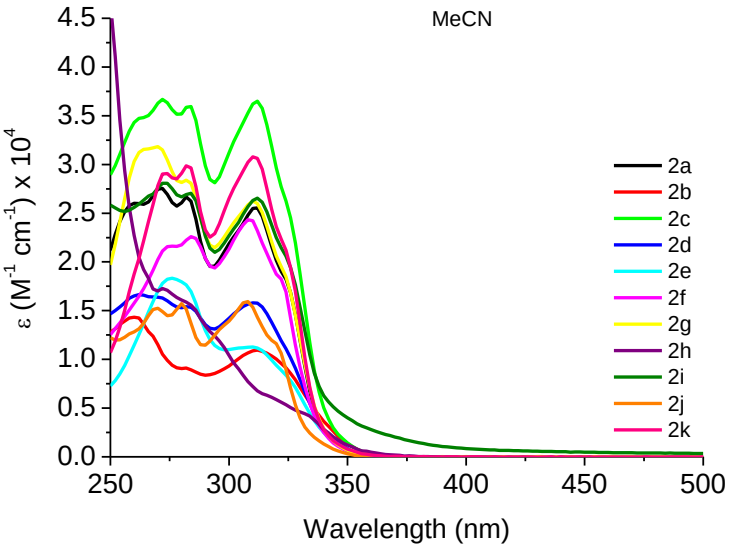

Figure S25. UV-Vis absorption spectra of coumarin derivatives **2a-2k** in MeCN (fixed concentration at 20 μM).

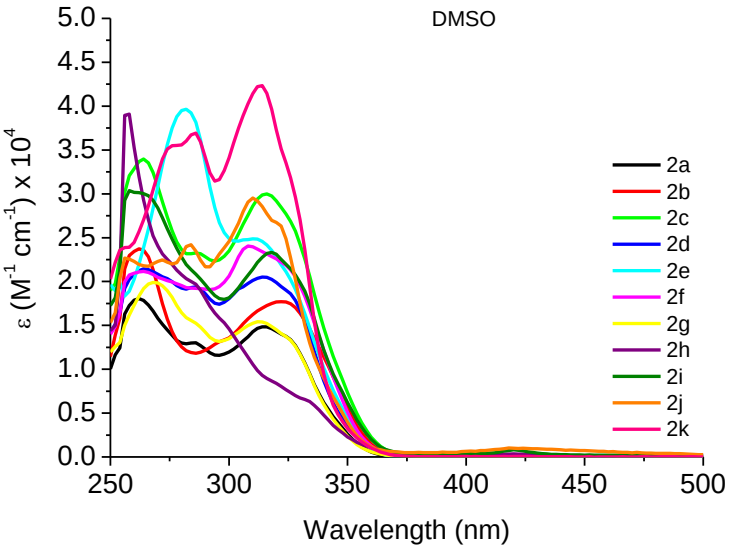

Figure S26. UV-Vis absorption spectra of coumarin derivatives **2a-2k** in DMSO (fixed concentration at 20 μM).

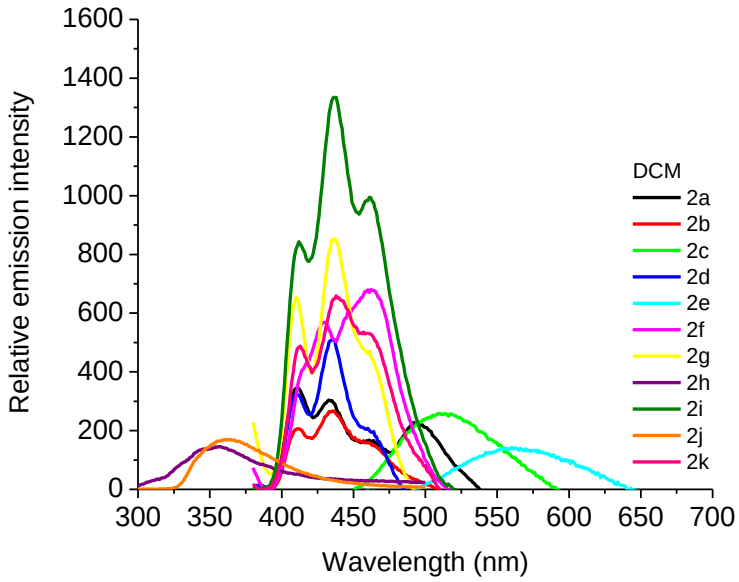

Figure S27. Steady-state fluorescence emission spectra of coumarin derivatives **2a-2k** in DCM (fixed concentration at 20 μM).

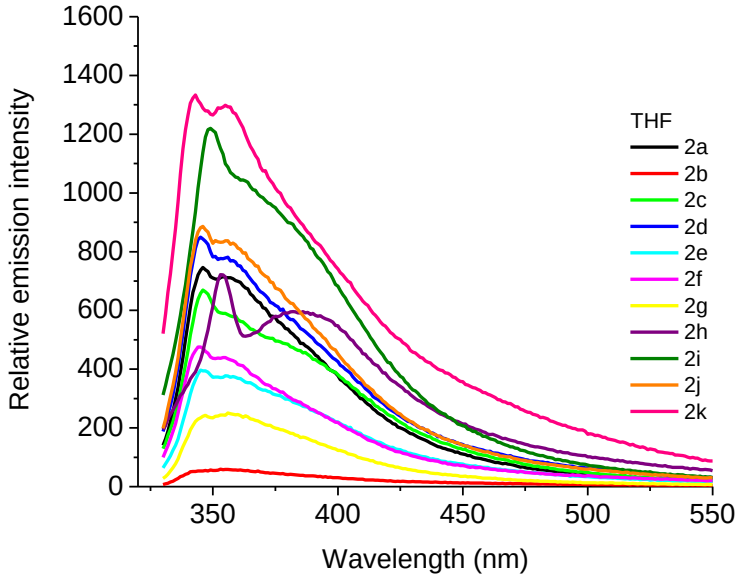

Figure S28. Steady-state fluorescence emission spectra of coumarin derivatives **2a-2k** in THF (fixed concentration at 20 μM).

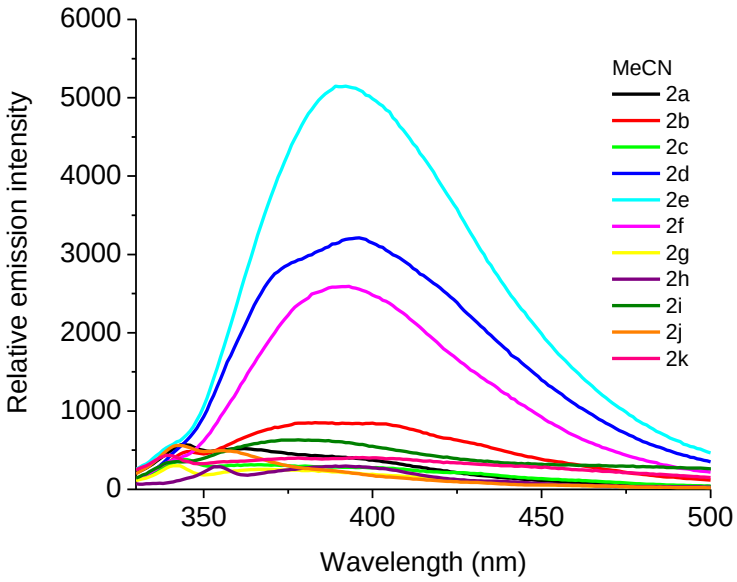

Figure S29. Steady-state fluorescence emission spectra of coumarin derivatives **2a-2k** in MeCN (fixed concentration at 20 μM).

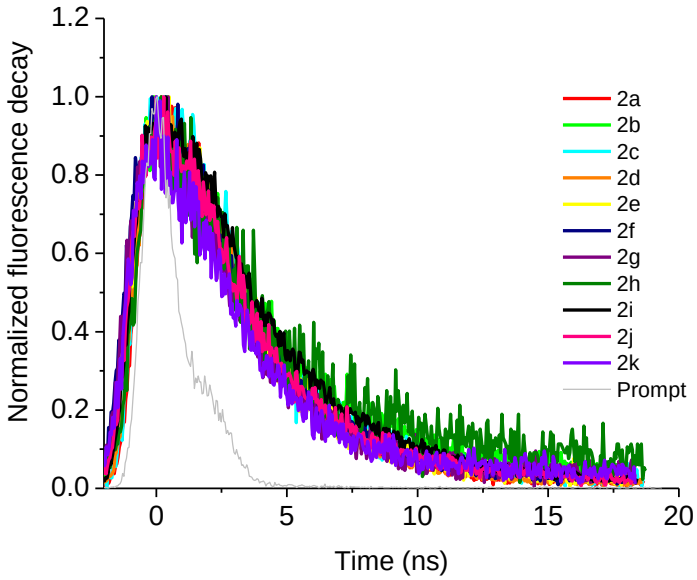

Figure S30. Normalized fluorescence decay plots of coumarin derivatives **2a-2k** in DMSO, using NanoLED at 284 nm as excitation source (fixed concentration at 20 μM).

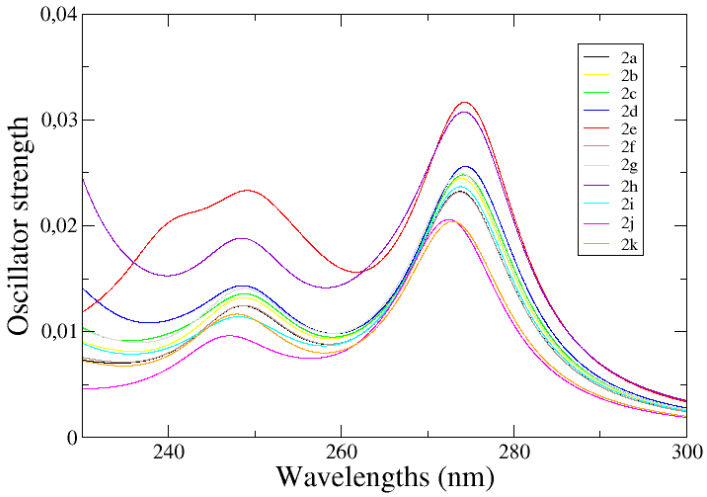

Figure S31. Theoretical absorption spectra of coumarin derivatives **2a-2k** in DMSO, by DFT analysis.

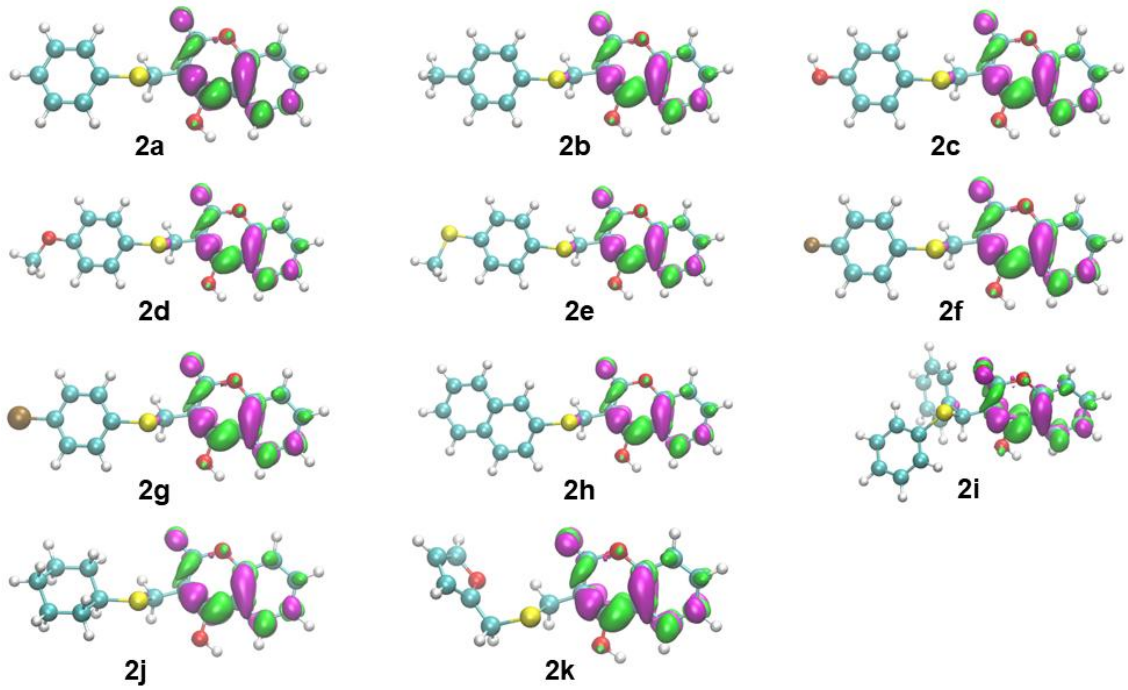

Figure S32. Electron density difference between the first excited state and the ground state of compounds **2a-2k**.

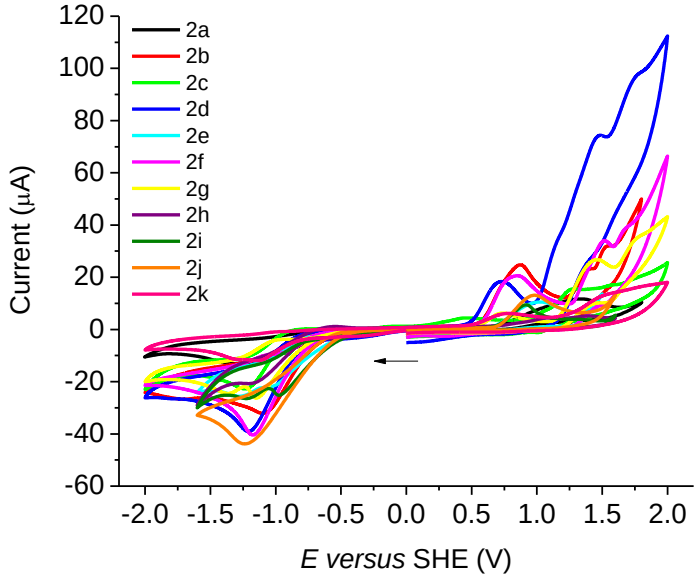

Figure S33. CV plots of coumarin derivatives **2a-2k** in DCM solution, using $TBAPF_6$ 0.1 M as supporting electrolyte, at scan rate of 100 mV s^{-1}.

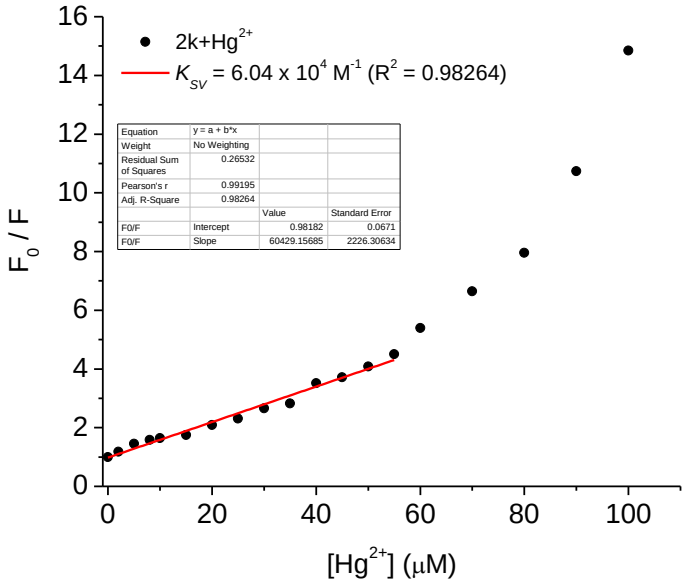

Equation	y = a + b*x		
Weight	No Weighting		
Residual Sum of Squares	0.26532		
Pearson's r	0.99195		
Adj. R-Square	0.98264		
		Value	Standard Error
F0/F	Intercept	0.98182	0.0671
F0/F	Slope	60429.15685	2226.30634

Figure S34. Stern-Volmer quenching (K_{SV}) plot between compound **2k** and Hg^{II} ions by steady-state fluorescence emission analysis.

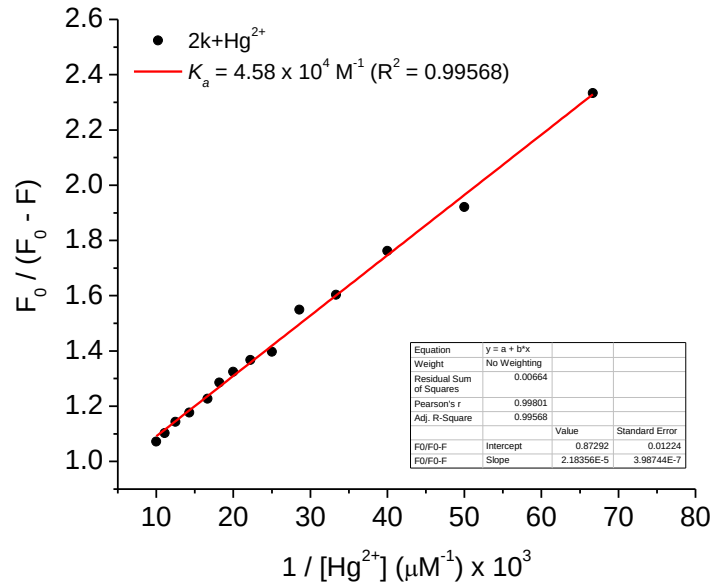

Figure S35. Association constant (K_a) plot between compound **2k** and Hg^{II} ions by steady-state fluorescence emission analysis.

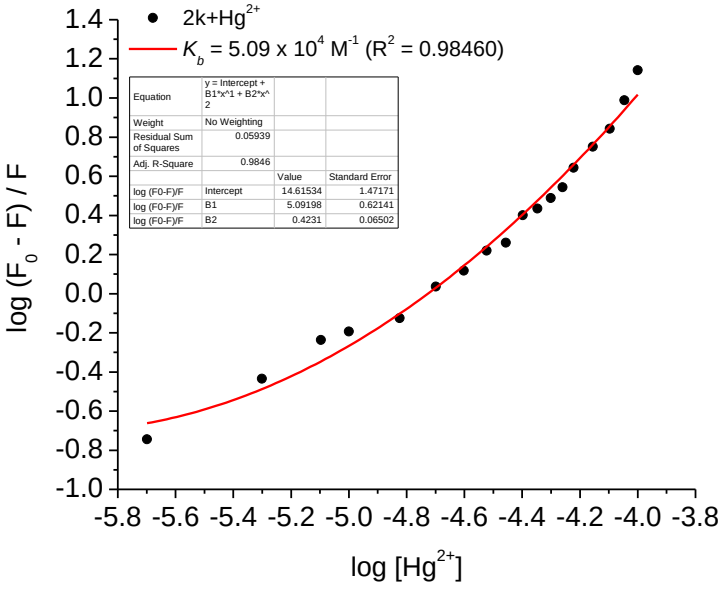

Figure S36. Binding constant (K_b) plot between compound **2k** and Hg^{II} ions by steady-state fluorescence emission analysis.

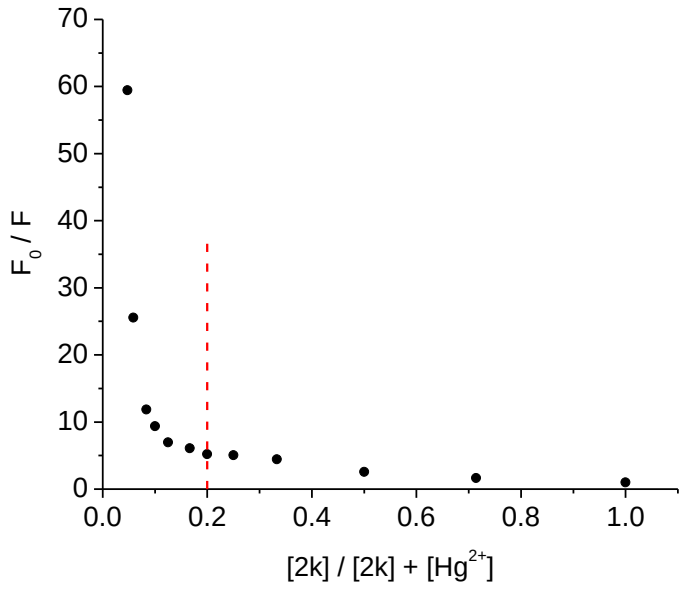

Figure S37. Job plots of coumarin derivatives **2k** with Hg^{2+} ion.

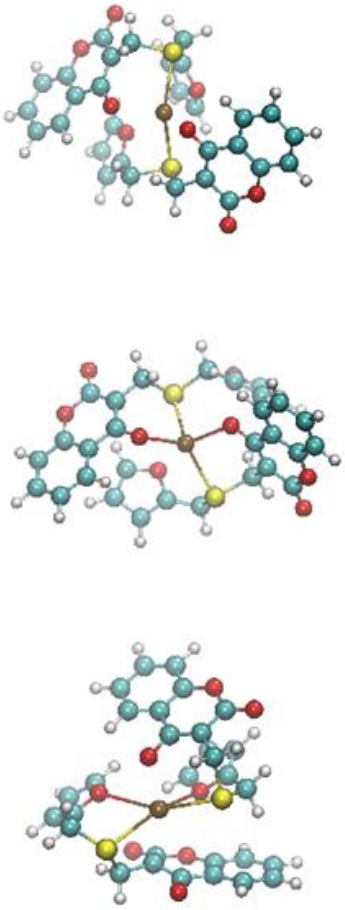

Figure S38. Optimized structures of the Hg^{2+}-**2k.** In the top panel, the Hg^{2+} bounds to the S atoms only. In the middle panel, the Hg^{2+} bounds to the S atoms and the O atoms of the coumarin moiety. In the bottom panel, the Hg^{2+} bounds to the S atoms and two O atoms from the furyl ring.

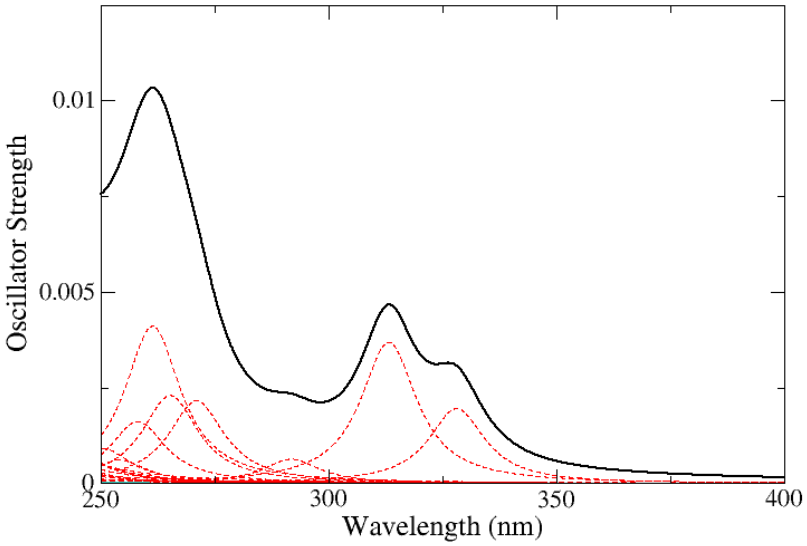

Figure S39. TDDFT absorption spectrum of the most stable structure of the Hg^{2+}-**2k** complex. The black solid line is the total spectrum, and the red dashed lines show the contributions of individual electronic transitions.

Table S1. Some examples of coumarin derivatives with Hg^{2+} detection

Coumarin structure	LOD (technique)
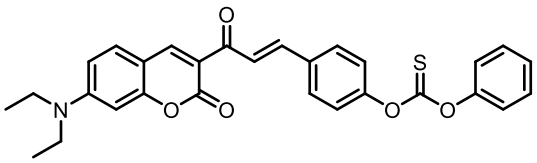	24.6 nM (emission)[1]
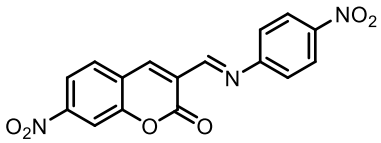	36.75 nM (emission)[2]
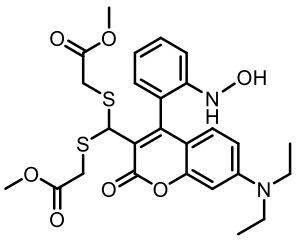	0.81 ppb (emission)[3]
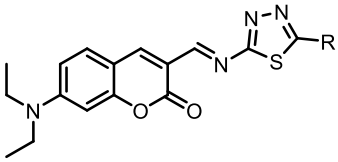	41.0 μM (emission)[4]
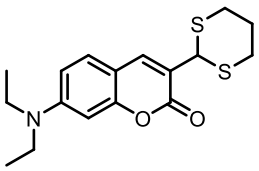	27.8 nM (emission)[5]

LOD: limit of detection.

Table S2. Electric dipole moments, in Debye, of the ground (μ_{GS}) and excited states (μ_{EX}) involved in the lowest energy electronic transitions of the absorption spectra

Compound	μ_{GS} / D	μ_{EX} / D
2a	8.25	6.05
2b	7.91	5.69
2c	6.69	4.36
2d	9.30	7.04
2e	9.50	7.14
2f	9.35	7.19
2g	9.84	7.69
2h	8.12	5.90
2i	10.42	8.08
2j	7.61	5.37
2k	7.96	5.69

References

1. He, S.-D.; Liu, Y.-L.; Ran, Y.-Y.; Mao, D.; Mou, C.-L.; Zuo, X.-L.; Zou, J.; Wu, C.; *J. Mol. Struc.* **2025**, *1342*, 142794. [Crossref]

2. Abbas, W. R.; Kadhim, M. A.; *RSC Adv.* **2025**, *15*, 44611. [Crossref]

3. Ding, Y.; Pan, Y.; Han, Y.; *Ind. Eng. Chem. Res.* **2019**, *58*, 7786. [Crossref]

4. Azhar, S.; Alam, M. Z.; Alimuddin; Khan, S. A.; *Inorg. Chim. Acta* **2025**, *588*, 122875. [Crossref]

5. Huang, L.; Sheng, W.; Wang, L.; Meng, X.; Duan, H.; Chi, L.; *RSC Adv.* **2021**, *11*, 23597. [Crossref]